

Gate Effects in a Hexagonal Zinc-Imidazolate-4-amide-5-imidate Framework with Flexible Methoxy Substituent and CO₂ Selectivity

Suvendu Sekhar Mondal,^a Asamanjoy Bhunia,^b Igor A. Baburin,^c Christian Jäger,^d Alexandra Kelling,^a Uwe Schilde,^a Gotthard Seifert,^c Christoph Janiak^b and Hans-Jürgen Holdt*^a

^a *Institut für Chemie, Anorganische Chemie, Universität Potsdam, Karl-Liebknecht-Straße 24-25, 14476 Potsdam, Germany. E-mail: holdt@uni-potsdam.de*

^b *Institut für Anorganische Chemie und Strukturchemie, Heinrich-Heine-Universität Düsseldorf, 40204 Düsseldorf, Germany*

^c *Institut für Physikalische Chemie und Elektrochemie, Technische Universität Dresden, 01062 Dresden, Germany*

^d *BAM Federal Institute for Materials Research and Testing, 12489 Berlin, Germany*

Supporting Information

21 pages

Experimental Details

Synthesis of IFP-7 was performed in seal tube from Ace Glass. All reagents and solvents were used as purchased from great chemical suppliers without further purification if not stated otherwise.

The linker precursors 2-methoxy-4,5-dicyanoimidazole (1)^{1a} and IFP-1^{1b} were synthesized following published procedure.

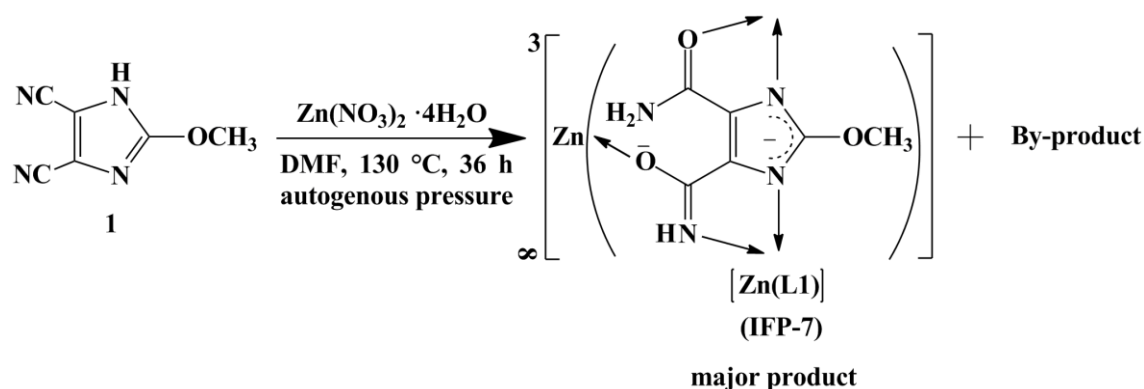
Elemental analysis (C, H, N) was performed on Elementar Vario EL elemental analyzer.

Synthesis of IFP-7

In a sealed tube (Typ A, company: Ace) 2-methoxy-4,5-dicyanoimidazole (**1**) (0.1 g, 0.76 mmol) and Zn(NO₃)₂ · 4H₂O (0.19 g, 0.76 mmol) were solved in DMF (6 mL). The sealed tube was closed and the mixture was heated at 130 °C for 36 hours and was then allowed to cool down to room temperature with 5 °C per hour. Afterwards, large amount of powder of was obtained along with some by-product formed at the inner wall of sealed tube. By-product is bigger in size. IFP-7 was separated by sieving technique,² which is used extensively in the mining industry and for determining particle size. Minor by-product (~ 10 %) was trapped by a mesh while IFP-7 (~ 90 %) filtered through it. We could not able to define the structure of the by-product, till now. Powder material was collected by filtration, washed with DMF and EtOH and dried in air. The material named as IFP-7.

After several attempts, we could not find a suitable crystal of IFP-7 for single X-ray diffraction.

IFP-7: Yield: ~ 67 % based on Zn(NO₃)₂ · 4H₂O; ¹³C CP-MAS NMR: δ =170.1, 167.2, 157.1, 132.7, 126.9, 55.7 ppm; Elemental analysis of activated IFP-7: C₆H₆N₄O₃Zn; Calcd., C 29.11, H 2.44, N 22.64; Found: C 29.27, H 2.31, N 26.76; IR (KBr pellet): ν_{max} = (3339 m, 3107 m, 1658 s, 1562 vs, 1478 m, 1285 m, 1252 m, 1220m, 1111 m, 795 m, 737 m) cm⁻¹.



Scheme S1. Synthesis of IFP-7.

Transformation of IFP-7 to the monomeric Zn-complex $[\text{Zn(L2)}_2(\text{H}_2\text{O})]$ (2)

5 mL H_2O was added in a sealed tube (Typ A, company: Ace), containing IFP-7 (0.1 g). The sealed tube was closed and the mixture was heated at 100°C for 36 hours and was then allowed to cool down to room temperature. Crystals were formed. Crystals were washed with EtOH and dried in air.

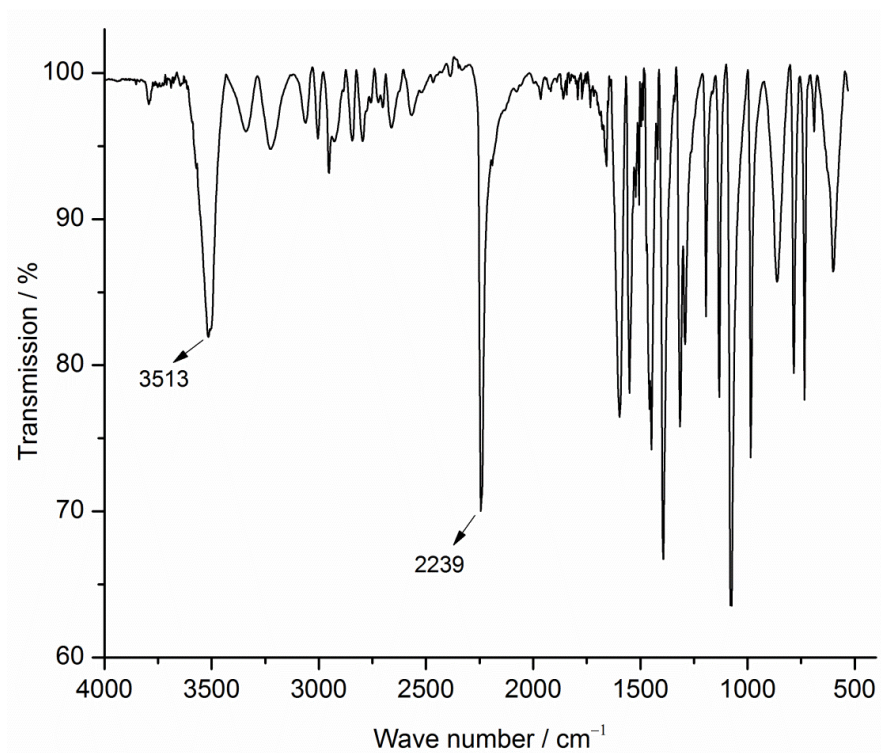
Yield: ~ 51 %, Elemental analysis of 2: $\text{C}_{12}\text{H}_{20}\text{N}_8\text{O}_9\text{Zn}$: Calcd., C 29.67, H 4.15, N 23.07, Found: C 29.58, H 4.31, N 23.22; IR (KBr pellet): $\nu_{\text{max}} = (3443 \text{ m}, 3335 \text{ m}, 1651 \text{ s}, 1593 \text{ vs}, 1475 \text{ m}, 1272 \text{ m}, 1103 \text{ m}, 1011 \text{ m}, 723 \text{ m}) \text{ cm}^{-1}$.

IR spectra

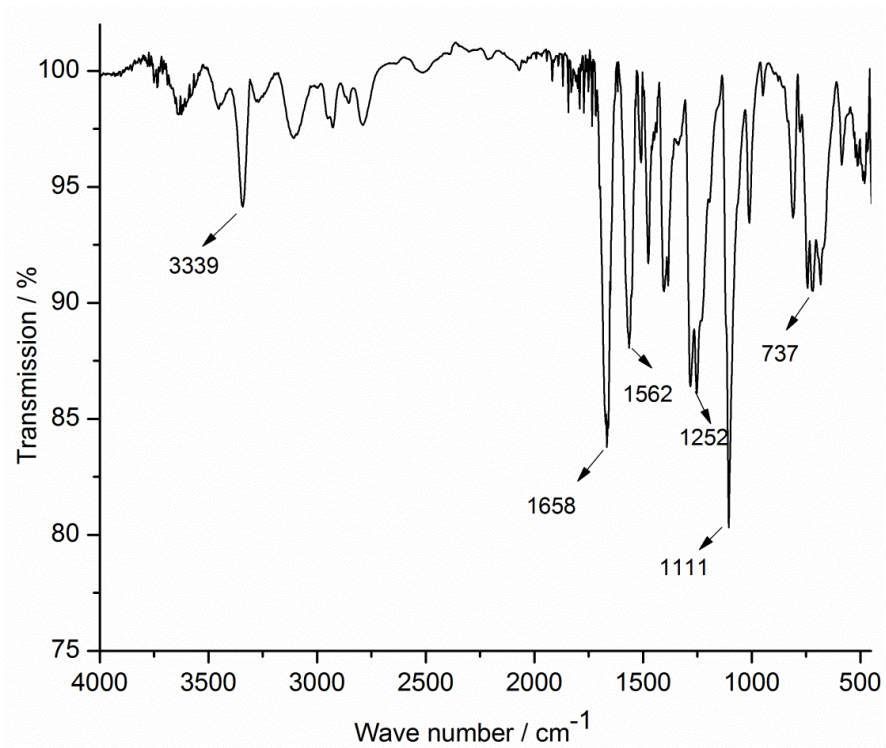
IR spectra were recorded on FT-IR Nexus from Thermo Nicolet in the region of $4000 - 400 \text{ cm}^{-1}$ using KBr pellets as basis.

The fabrication of framework comes from IR stretch that no stretching bands related to $\text{C}\equiv\text{N}$ in the region of $2230\text{--}2240 \text{ cm}^{-1}$. Instead, new typical bands for amide and imidate groups observed between $3100\text{--}3350 \text{ cm}^{-1}$ and at $1560\text{--}1660 \text{ cm}^{-1}$.

A)



B)



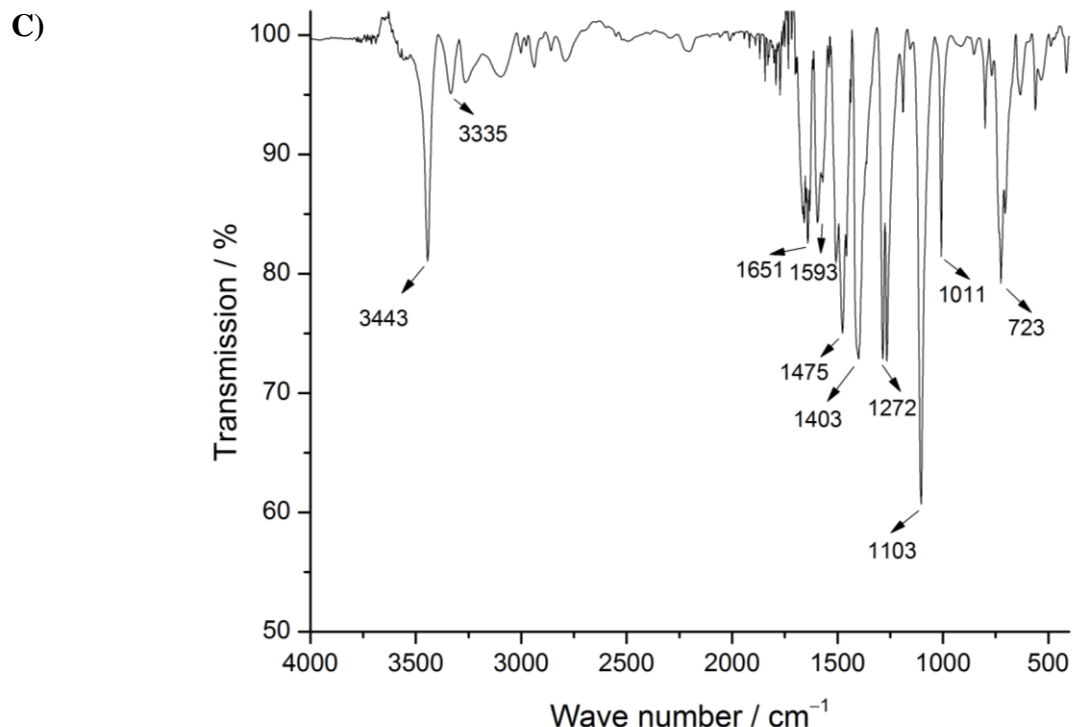


Fig. S1: IR-spectra of: **A)** 2-Methoxy-4,5-dicyanoimidazole (1); **B)** IFP-7 as-synthesized; **C)** Zn-complex $[\text{Zn}(\text{L2})_2(\text{H}_2\text{O})]$ (2).

^1H and ^{13}C CPMAS NMR Spectroscopy

^1H and ^{13}C Cross Polarization experiments with Magic Angle Sample Spinning (^{13}C CPMAS NMR) for IFP-7 was performed on a Bruker Avance 600 spectrometer (Bruker Biospin GmbH, Rheinstetten, Germany, $B_0 = 14.1$ T) operating at a frequency of 150.9 MHz using a double resonant 4 mm MAS (magic angle sample spinning) probe. The spinning frequency was 12.5 kHz. For CP, a ramped (50 % ramp) lock field was used on the ^1H channel with a CP contact time of 2 ms, a recycle delay of 3 s and 512 scans. The 90° ^1H pulse length was 3.3 μs . High power TPPM decoupling was applied ($B_1 = 80$ kHz). The ^{13}C chemical shifts are referenced using the glycine carboxyl group signal ($\delta(^{13}\text{C}) = 176.4$ ppm).

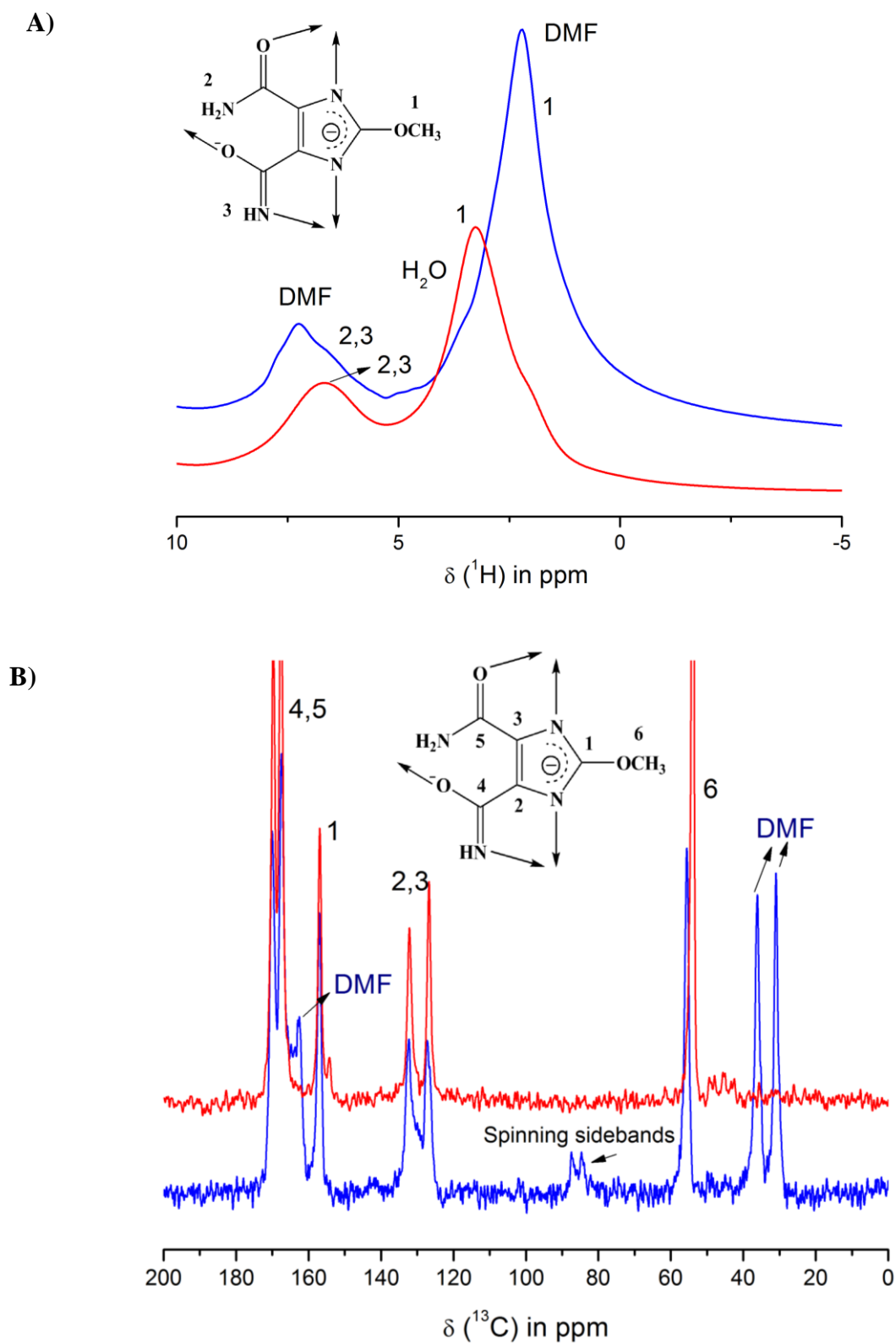


Fig. S2: ^1H - **A)** and ^{13}C - **B)** CP-MAS NMR spectra of IFP-7 (blue – as-synthesized, red – activated), activation procedure: 200°C and 10^{-3} mbar, 30 hrs.

Theoretical calculations of crystal structure of IFP-7

DFT calculations (PBE functional³) were performed by using the SIESTA program package.⁴ The DZP basis set used in the calculations was first tested on the structure of IMOF-3 (later, we named IMOF-3 as IFP-1) solved from single-crystal X-ray data,^{1b} and showed very good agreement with respect to unit cell parameters (compare $a_{\text{calcd}} = 17.5313 \text{ \AA}$ and $c_{\text{calcd}} = 18.6286 \text{ \AA}$ vs. $a_{\text{exptl}} = 17.9244 \text{ \AA}$ and $c_{\text{exptl}} = 18.4454 \text{ \AA}$), bond lengths and angles. Due to the large unit cell sizes, it was sufficient to include only the Γ -point of the Brillouin zone for the evaluation of integrals in the reciprocal space.

Powder X-ray-diffraction patterns

Powder X-ray diffraction (PXRD) patterns of all IFPs were measured on a Siemens Diffractometer D5005 in Bragg-Brentano reflection geometry. The diffractometer was equipped with a copper tube, a scintillation counter, automatical incident- and diffracted-beam soller slits and with a graphite secondary monochromator. The generator was set to 40 kV and 40 mA. All measurements were performed with sample rotating. Data were collected digitally from 3° to 70° 2θ using a step size of 0.02° 2θ and a count time of 4 seconds per step. The simulated powder patterns for IFP-7 were calculated using single-crystal X-ray diffraction data and processed by the free Mercury v1.4.2 program provided by the Cambridge Crystallographic Data Centre.

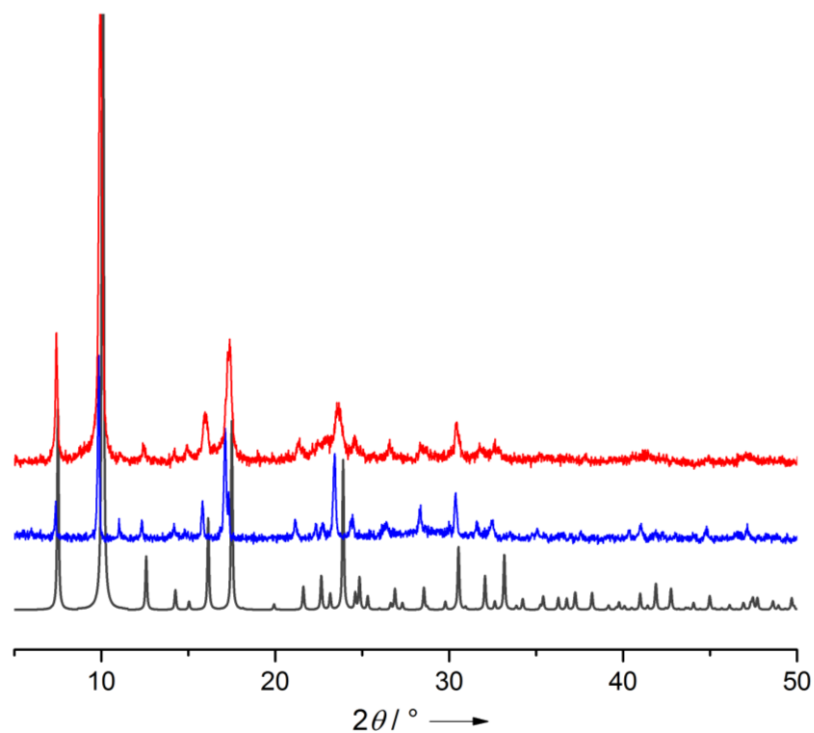


Fig. S3: Powder X-ray diffraction patterns of IFP-7 (Color: black = simulated, blue = As-synthesized IFP-7, red = Activated).

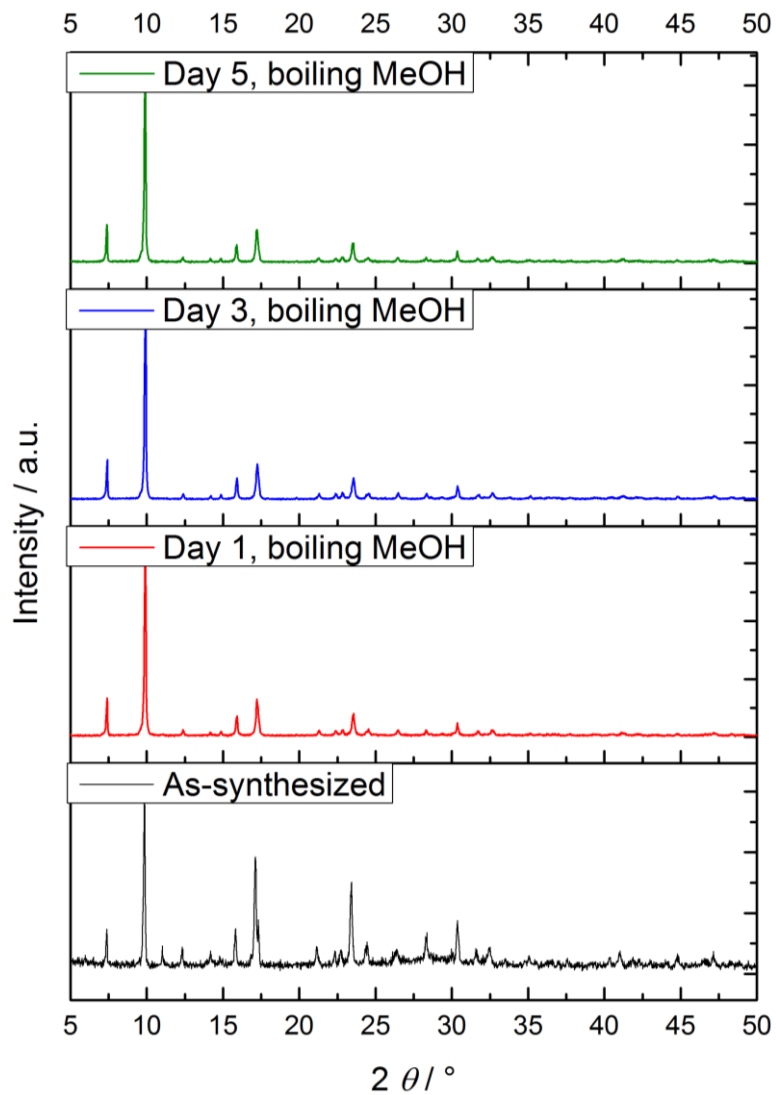


Fig. S4: Powder X-ray diffraction profiles of IFP-7, collected during stability tests in refluxing methanol.

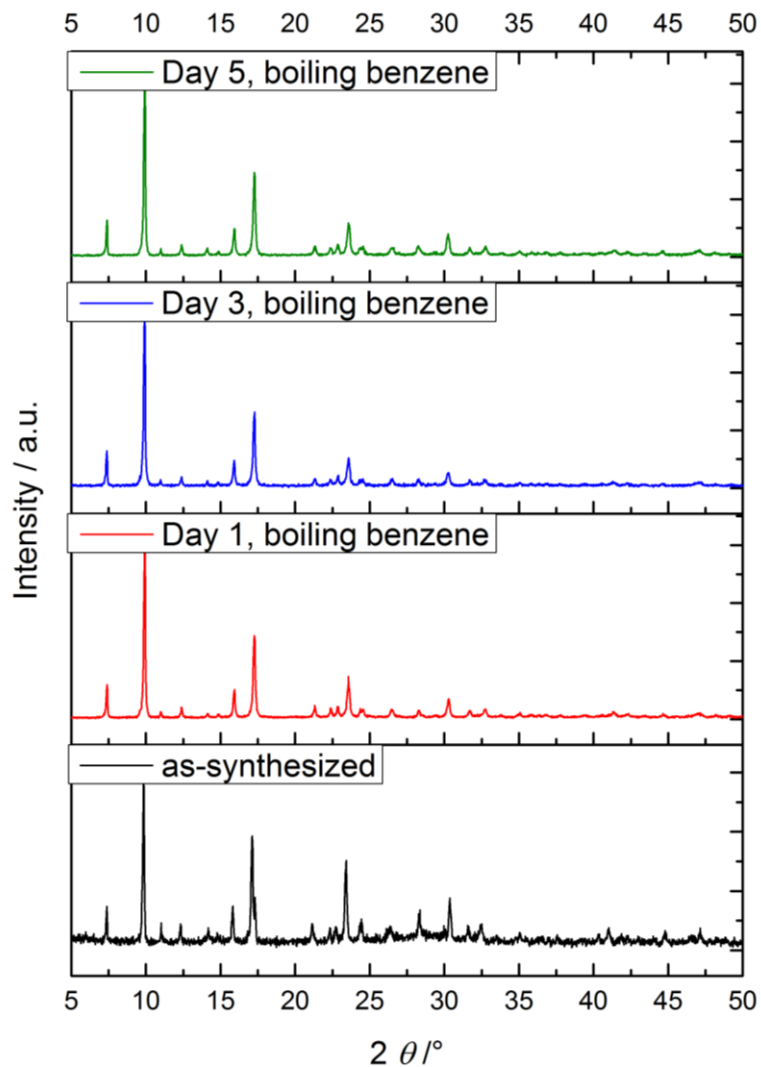


Fig. S5: Powder X-ray diffraction profiles of IFP-7, collected during stability tests in refluxing benzene.

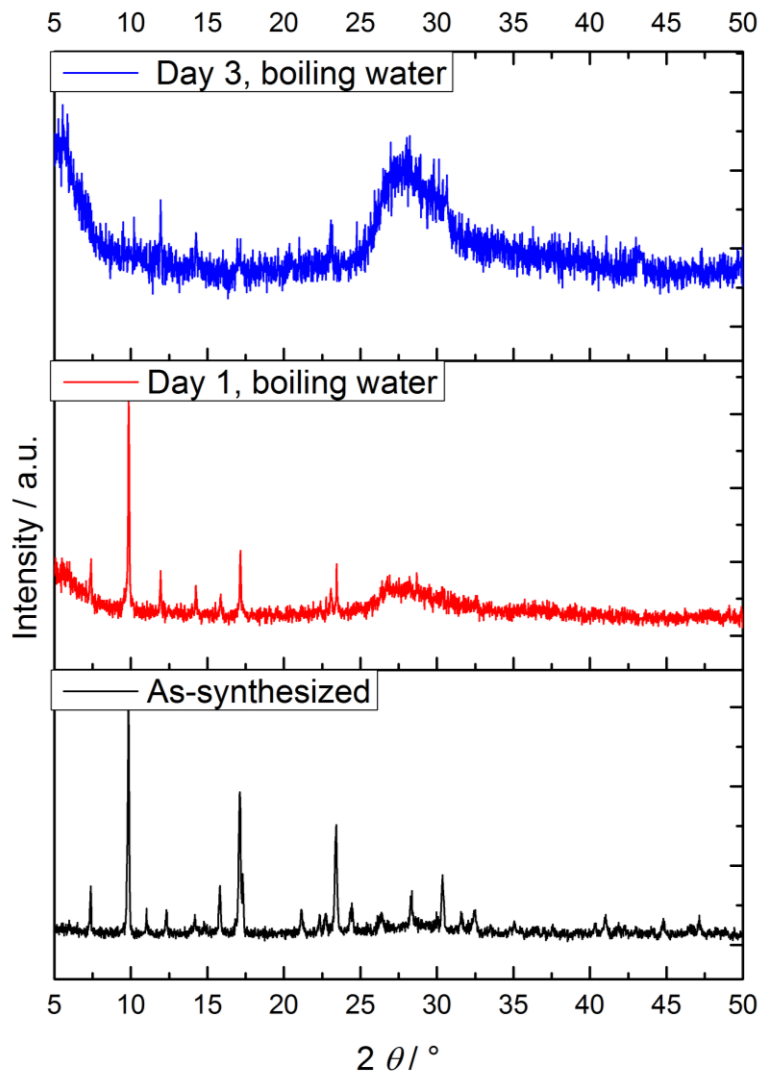


Fig. S6: Powder X-ray diffraction profiles of IFP-7, collected during stability tests in refluxing water.

Single crystal X-ray structure determination of monomeric Zn-complex [Zn(L2)₂(H₂O)] (2)

The crystal was embedded in perfluoropolyalkylether oil and mounted on a glass fibre. Intensity data were collected at 150 K using a STOE Imaging Plate Diffraction System IPDS-2 with graphite monochromatized MoK α radiation ($\lambda = 0.71073 \text{ \AA}$) at 50 kV and 40 mA (360 frames, $\Delta\omega=1^\circ$, 2 min exposure time per frame). The data were corrected for Lorentz polarization and absorption effects. The structure was resolved with direct methods using SHELXS-97⁵ and

refined with full-matrix least-squares on F^2 using the program SHELXL-97.⁶ All non-hydrogen atoms were refined anisotropically.

The hydrogen atoms of the methyl groups were calculated in their expected positions and refined as riding atoms with $U_{\text{iso}}(\text{H}) = 1.5 U_{\text{eq}}(\text{C})$.

The other hydrogen atoms were located from the difference Fourier map and refined with $U_{\text{iso}}(\text{H}) = 1.5 U_{\text{eq}}(\text{N}, \text{O})$.

Table S1. Selected crystallographic data and details of the structure refinements of monomeric Zn-complex $[\text{Zn}(\text{L2})_2(\text{H}_2\text{O})]$ (2).

Chemical formula	$\text{C}_{12}\text{H}_{20}\text{N}_8\text{O}_9\text{Zn}$
Formula Mass	485.73
Crystal system	triclinic
Space group	$P\bar{1}$
$a/\text{\AA}$	8.7253(6)
$b/\text{\AA}$	9.1928(6)
$c/\text{\AA}$	12.6864(8)
$\alpha/^\circ$	98.872(5)
$\beta/^\circ$	100.538(5)
$\gamma/^\circ$	109.715(5)
Unit cell volume/ \AA^3	915.78(11)
Temperature/K	150
No. of formula units per unit cell, Z	2
Radiation type	MoK α
Absorption coefficient, μ/mm^{-1}	1.411
Reflections collected	11907
No. of independent reflections	3230
R_{int}	0.0184
R_1 / wR_2 [$I > 2\sigma(I)$]	0.0210 / 0.0595
R_1 / wR_2 (all data)	0.0222 / 0.0601
Goodness of fit on F^2	1.064

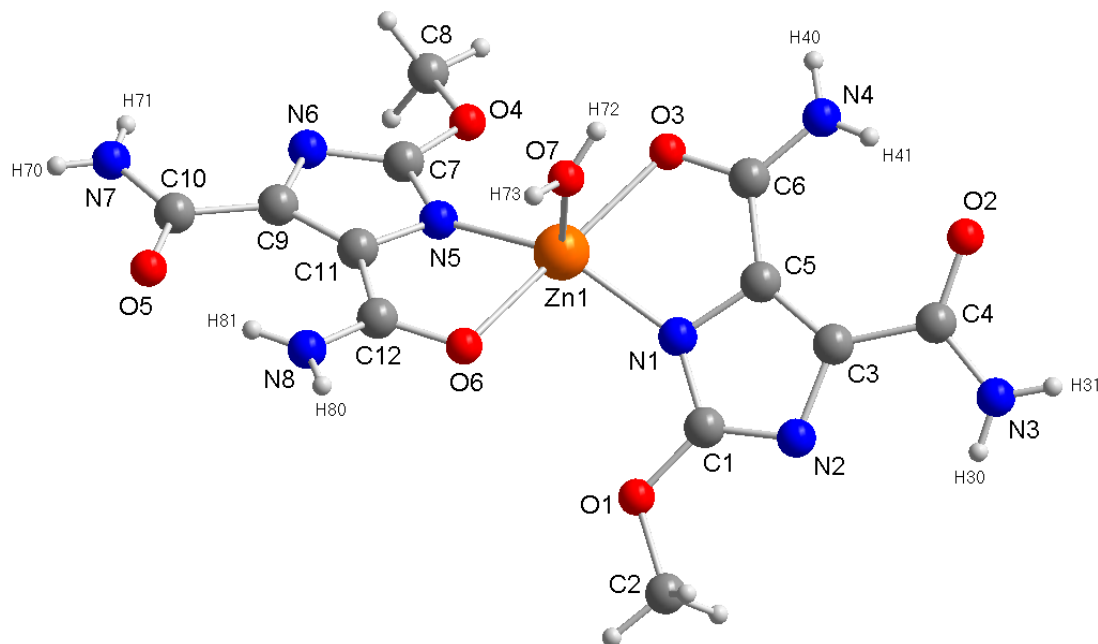


Fig. S7: Crystal structure of monomeric Zn-complex $[\text{Zn}(\text{L2})_2(\text{H}_2\text{O})]$ (2) showing the coordination environment of Zn^{II} and the coordination mode of the ligand 2-methoxyimidazolate-4,5-diamide (L2). Non-coordinating water molecules are omitted for clarity.

Zn^{2+} ion is pentacoordinated by donor atoms of two ligands (4,5-diamide-2-methoxyimidazolate). Ligand L1 in IFP-7 is transformed to 2-methoxyimidazolate-4,5-diamide (L2) in refluxing water. Two imidazolate N atoms (N1 and N5), two amide O atoms (O3 and O6), and one O atom (O7) from water molecule formed a distorted environment with a square - pyramidal geometry. The packing is stabilized by a system of hydrogen bonds. For structural parameters as bond lengths, bond angles, and hydrogen bonds – see cif.

CCDC-925826 of $[\text{Zn}(\text{L2})_2(\text{H}_2\text{O})]$ (2) contains the supplementary crystallographic data for this paper. These data can be obtained free of charge from The Cambridge Crystallographic Data Centre via www.ccdc.cam.ac.uk/data_request/cif.

Thermogravimetric (TG) analysis

The TG measurements were performed in a stationary air atmosphere (no purge) from room temperature up to 800 °C using a Linseis thermal analyzer (Linseis, Germany) working in the vertical mode. The heating rate was 10 °C/min. The samples were placed in cups of aluminium oxide.

Thermogravimetric analysis (TGA) trace for as-synthesized IFP-7 indicated a gradual weight-loss of 12 % (25–250°C), corresponding to partial loss of guest species like water molecules and *N,N'*-dimethylformamide (DMF), followed by the decomposition of framework. Activated sample shows the thermal stability up to 300 °C.

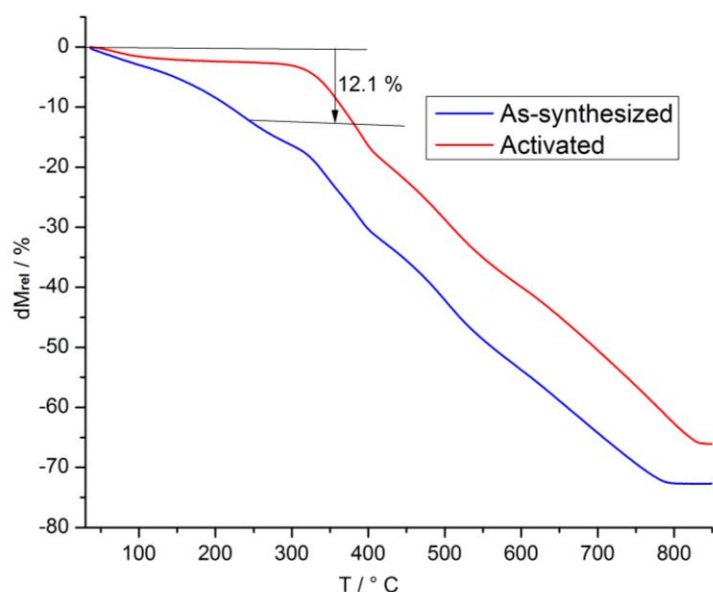


Fig. S8: TGA curves of as-synthesized (color: blue) and activated compound (color : red) IFP-7.

Gas-sorption measurements

The sample was connected to the preparation port of the sorption analyzer and degassed under vacuum until the out gassing rate, i.e., the rate of pressure rise in the temporarily closed manifold with the connected sample tube, was less than 2 $\mu\text{Torr}/\text{min}$ at the specified temperature 160 $^{\circ}\text{C}$ for 24 h. After weighing, the sample tube was then transferred to the analysis port of the sorption analyzer. All used gases (H_2 , He, N_2 , CO_2 , CH_4) were of ultra high purity (UHP, grade 5.0, 99.999%) and the STP volumes are given according to the NIST standards (293.15 K, 101.325 kPa). Helium gas was used for the determination of the cold and warm free space of the sample tubes. H_2 and N_2 sorption isotherms were measured at 77 K (liquid nitrogen bath), whereas CO_2 and CH_4 sorption isotherms were measured at 298 ± 1 K (passive thermostating) 273.15 K (ice/deionized water bath) and 195.0 K (acetone/dry ice). The heat of adsorption values and the DFT calculations (' N_2 DFT slit pore' model) were done using the ASAP 2020 v3.05 software.

H_2 uptake

To check the hysteresis, we have measured the H_2 uptake capacity of a freshly prepare sample at 77 K by increasing the equilibrium time.

Table S2 summarizes the equilibrium time interval, measurement time and H_2 uptake for IFP-7. The H4 type hysteresis is mostly caused by irreversible uptake of molecules in pores (or through pore entrances).⁷ We have increased the equilibration interval up to 50 s which had taken the measurement time 68 h. If we further increased the equilibration interval, then it will be a problem to keep the temperature constant (77 K).

Table S2. H₂ uptake measurements at different equilibrium time interval.

Condition		Curve or Experiment	Measurement time (h)	H ₂ uptake (cm ³ /g) ^a
Absolute pressure (mmHg)	Equilibration Interval ^b (s)			
0-50	20	curve or experiment 1	IFP-7: 29 IFP-1: 8	35
50-500	15			
500-1000	10			
0-50	30	curve or experiment 2	38	37
50-500	30			
500-1000	30			
0-50	50	curve or experiment 3	68	50
50-500	50			
500-1000	50			

^a H₂ uptake with a standard deviation of ± 15 cm³/g at 77 K and 1 bar.

^b Equilibration time allowed during both adsorption and desorption at each data point up in the stated pressure range

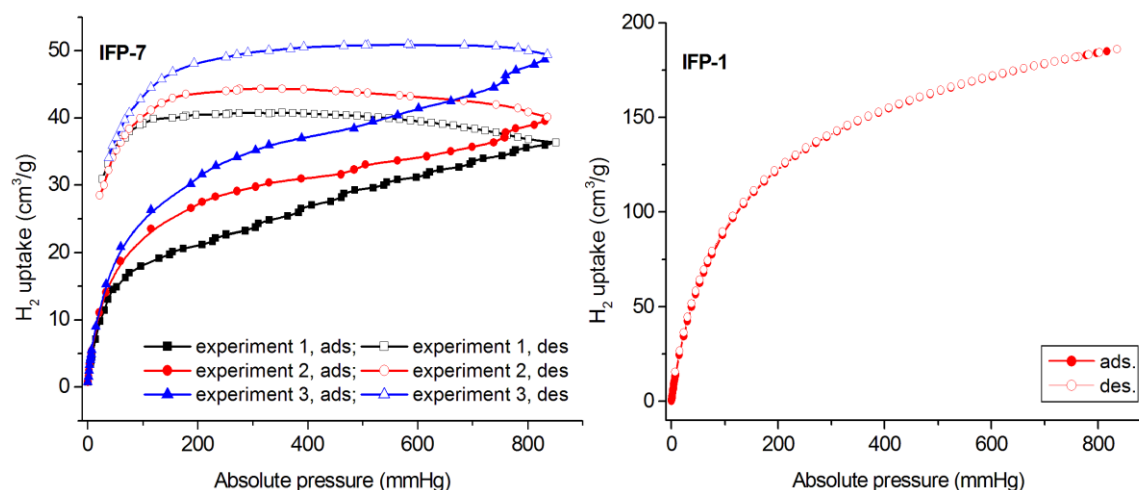


Fig. S9: H₂ gas sorption isotherms of IFP-7 under different equilibration interval. (left) and IFP-1 (right). Adsorption and desorption branches are indicated in closed and open symbols, respectively.

To compare the hysteresis of IFP-7, we measured the H₂ sorption at a similar condition (curve or exp.-1) for IFP-1 which is similar in structure to IFP-7 except for the methyl instead of a

methoxy group (IFP-1 contains a *methyl* group; IFP-7 contains a *methoxy* group, Fig. S10). In IFP-1, there is no hysteresis during the desorption (Fig. S9, right). Therefore, we confirmed that the equilibrium time interval is not a key issue for such broad hysteresis.

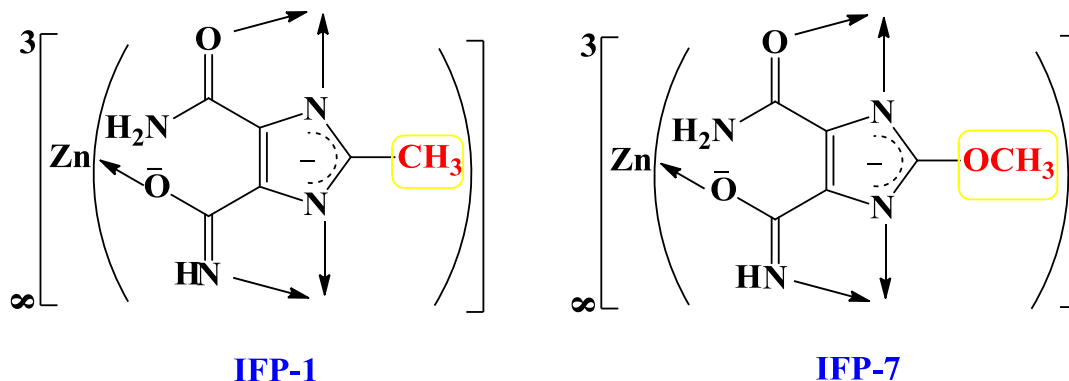


Fig. S10: Schematic structure of IFP-1 (left) and IFP-7 (right)

The broad desorption hysteresis for H₂ in IFP-7 does not change with the equilibrium time interval. This was also confirmed for the narrower desorption hysteresis of CO₂ at 273 K in IFP-7. At 273 K, again we observed the similar hysteresis when the ad- and desorption equilibrium time interval was increased to 50 s over the whole pressure range (Fig.S14).

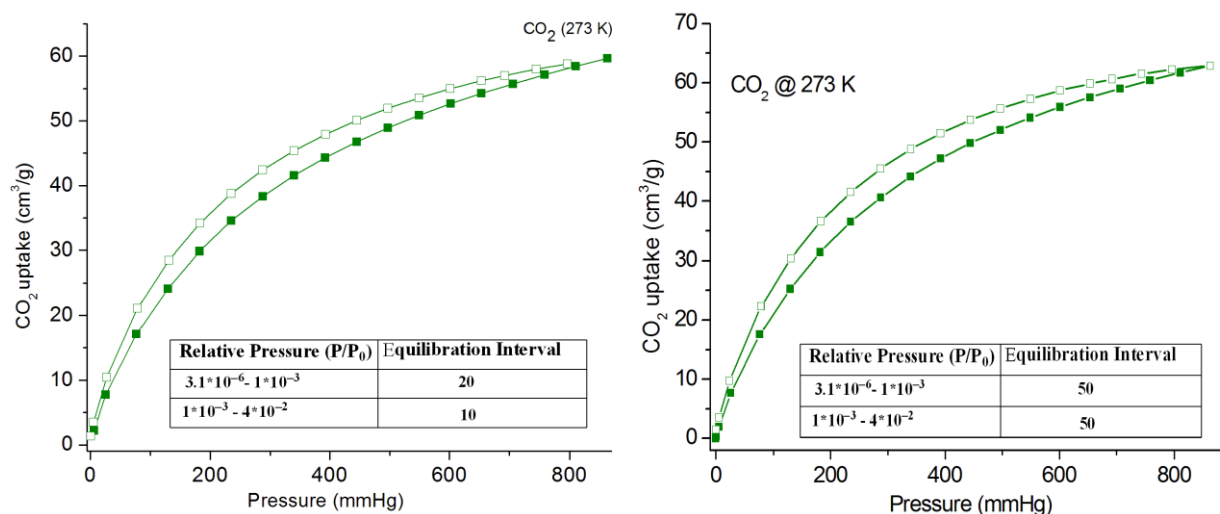


Fig. S11: CO₂ gas sorption isotherms of IFP-7 under different equilibration interval. Showing almost no change in hysteresis upon desorption.

Heat of adsorption

From two adsorption isotherms acquired at different temperatures T_1 and T_2 , the differential heat of adsorption $\Delta H_{ads,diff}$ can be calculated for any amount of adsorbed substance after determining the required relative pressures p_1 and p_2 . A modified form of the Clausius-Clapeyron equation is used (eq (1))⁸ $\Delta H_{ads,diff}$ was calculated over the whole adsorption range from the 273 K and 298 K isotherms for CO₂.

$$\Delta H_{ads,diff} = -R \ln\left(\frac{p_2}{p_1}\right) \frac{T_1 T_2}{T_2 - T_1} \quad (1)$$

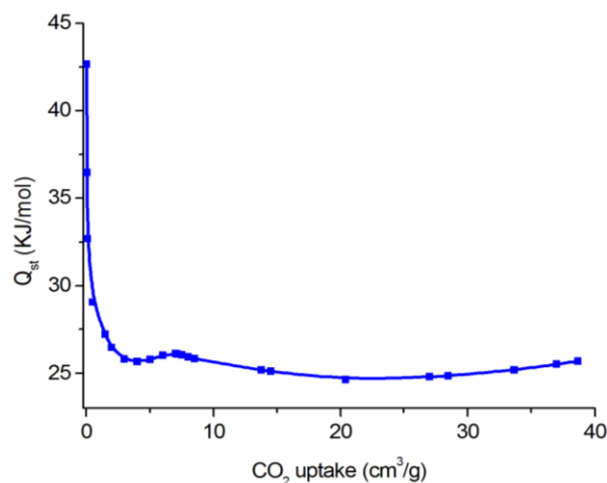


Fig. S12: Isosteric heats of CO₂ adsorption as a function of the adsorbent loading for IFP-7.

Selectivity

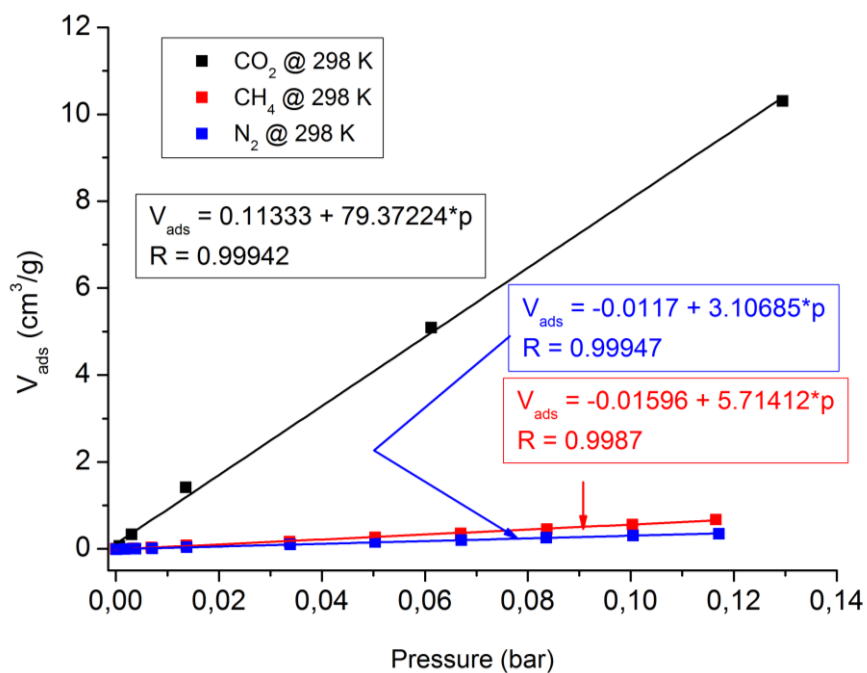


Fig. S13: The initial slope in the Henry region of the sorption isotherms of CO₂ (black) and CH₄ (red) and N₂ (blue) of IFP-7 at 298 K.

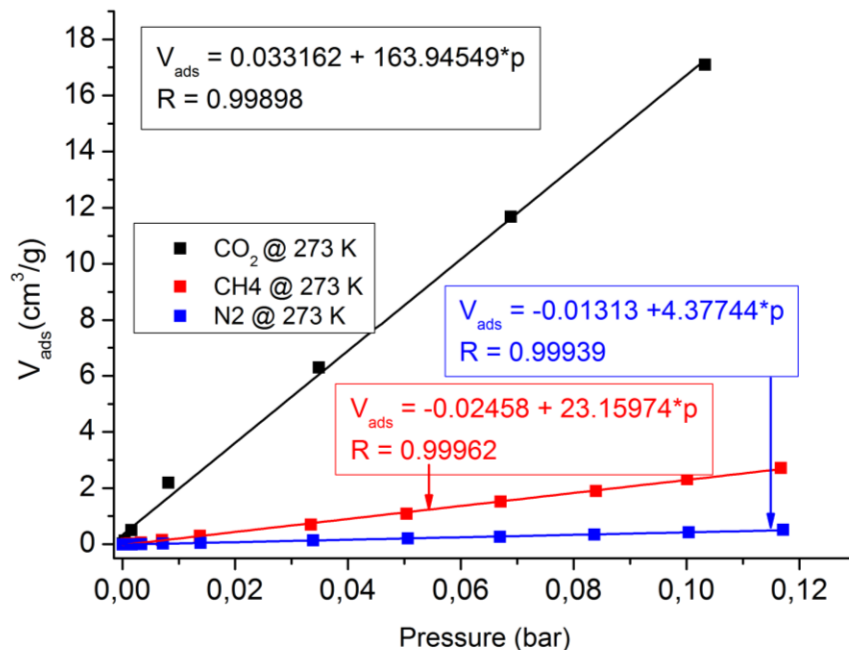


Fig. S14: The initial slope in the Henry region of the sorption isotherms of CO₂ (black) and CH₄ (red) and N₂ (blue) of IFP-7 at 273 K.

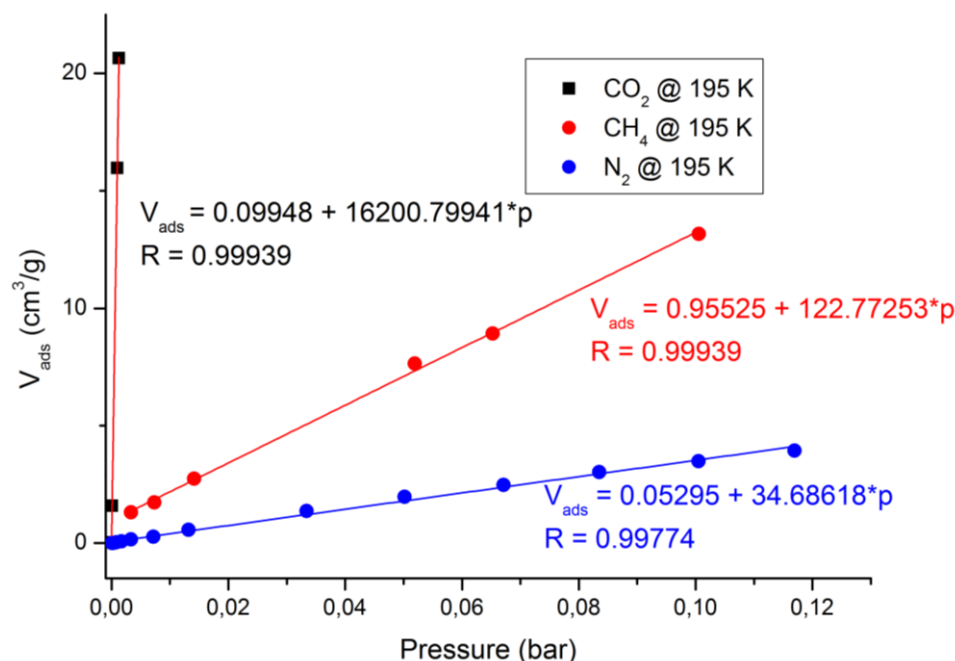


Fig. S15: The initial slope in the Henry region of the sorption isotherms of CO₂ (black) and CH₄ (red) and N₂ (blue) of IFP-7 at 195 K.

References

- (a) W. K. Anderson, D. Bhattacharjee, and D. M. Houston, *J. Med. Chem.*, 1989, **32**, 119–127;
(b) F. Debatin, A. Thomas, A. Kelling, N. Hedin, Z. Bacsik, I. Senkovska, S. Kaskel, M. Junginger, H. Müller, U. Schilde, C. Jäger, A. Friedrich and H.-J. Holdt, *Angew. Chem. Int. Ed.* 2010, **49**, 1258–1262.
- T. D. Keene, D. J. Price and C. J. Kepert, *Dalton Trans.*, 2011, **40**, 7122–7126.
- J. P. Perdew, K. Burke, M. Ernzerhof, *Phys. Rev. Lett.*, 1996, **77**, 3865–3868.
- J. M. Soler, E. Artacho, J. D. Gale, A. García, J. Junquera, P. Orde-jón and D. Sánchez Portal, *J. Phys.: Condens. Matter*, 2002, **14**, 2745–2779.
- Sheldrick, G. M. SHELXS-97 Program for the Crystal Structure Solution, University of Göttingen, Germany, 1997.
- Sheldrick, G. M. SHELXL-97 Program for the Crystal Solution Refinement, University of Göttingen, Göttingen, 1997.

7 (a) K. S. W. Sing, D. H. Everett, R. A. W. Haul, L. Moscou, R. A. Pierotti, J. Rouquerol and T. Siemieniewska, *Pure Appl. Chem.*, 1985, **57**, 603-619; (b) M. Thommes, B. Smarsly, M. Groenewolt, P. I. Ravikovitch and A. V. Neimark, *Langmuir* 2005, **22**, 756-764.

8 F. Rouquerol, J. Rouquerol and K. Sing, Adsorption by powders and porous solids, (F. Rouquerol, J. Rouquerol, K. Sing, Eds.), Academic Press, San Diego, 1999, vol. 11.